Published in final edited form as:

ACS Macro Lett. 2019 April 16; 8(4): 473–478. doi:10.1021/acsmacrolett.9b00016.

Polyoxazoline-Based Bottlebrush and Brush-Arm Star Polymers via ROMP: Syntheses and Applications as Organic Radical Contrast Agents

Gabriela Gil Alvaradejo[†,‡,§,‖], **Hung V.-T. Nguyen**[§,‖], **Peter Harvey**[⊥,#,○], **Nolan M. Gallagher**[§], **Dao Le**[†,‡], **M. Francesca Ottaviani**[□], **Alan Jasanoff**[⊥,#,○], **Guillaume Delaittre**[*,†,‡], and **Jeremiah A. Johnson**[*,§]

[†]Institute of Toxicology and Genetics (ITG), Karlsruhe Institute of Technology (KIT), Hermann-von-Helmholtz-Platz, 76134 Eggenstein-Leopoldshafen, Germany

[‡]Institute for Chemical Technology and Polymer Chemistry (ITCP), Karlsruhe Institute of Technology (KIT), 76128 Karlsruhe, Germany

[§]Department of Chemistry, Massachusetts Institute of Technology, Cambridge, Massachusetts 02139, United States

[⊥]Department of Biological Engineering, Massachusetts Institute of Technology, Cambridge, Massachusetts 02139, United States

[#]Department of Brain and Cognitive Sciences, Massachusetts Institute of Technology, Cambridge, Massachusetts 02139, United States

[○]Department of Nuclear Science and Engineering, Massachusetts Institute of Technology, Cambridge, Massachusetts 02139, United States

[□]Department of Pure and Applied Sciences, University of Urbino, Urbino 61029, Italy

Abstract

The synthesis of functional poly(2-alkyl-2-oxazoline) (PAOx) copolymers with complex nanoarchitectures using a graft-through ring-opening metathesis polymerization (ROMP) approach is described. First, well-defined norbornene-terminated poly(2-ethyl-2-oxazoline) (PEtOx) macromonomers (MM) were prepared by cationic ringopening polymerization. ROMP of these MMs produced bottlebrush copolymers with PEtOx side chains. In addition, PEtOx-based branched MMs bearing a terminal alkyne group were prepared and conjugated to an azide-containing bis-spirocyclohexyl nitroxide via Cu-catalyzed azide-alkyne cycloaddition (CuAAC). ROMP of this branched MM, followed by in situ cross-linking, provided PEtOx-based brush-arm star polymers (BASPs) with nitroxide radicals localized at the core-shell interface. These PEtOx-

[*]**Corresponding Authors:** guillaume.delaittre@kit.edu, jaj2109@mit.edu.

[‖]G.G.A. and H.V.-T.N. contributed equally.

Supporting Information

The Supporting Information is available free of charge on the ACS Publications website at DOI: 10.1021/acsmacrolett.9b00016. Materials, instrumentation, experimental procedures, NMR and mass spectra, additional SEC traces and EPR spectra with fitting data (PDF).

The authors declare no competing financial interest.

based nitroxide-containing BASPs displayed relaxivity values on par with state-of-the-art polyethylene glycol (PEG)-based nitroxide materials, making them promising as organic radical contrast agents for metal-free magnetic resonance imaging (MRI).

Graphical Abstract

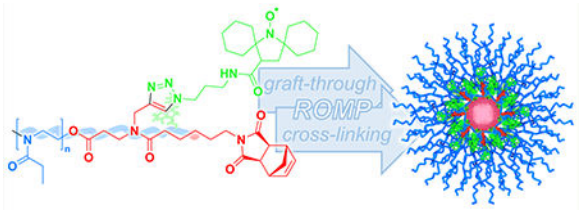

Particular members of the poly(2-alkyl/aryl-2-oxazoline) (PAOx) class of polymers, for example, poly(2-(m)ethyl-2-oxazoline)s,[1,2] have garnered increasing interest in the biomedical field. The unique properties of PAOx, such as biocompatibility and stealth behavior, make them potential alternatives to polyethylene glycol (PEG), the gold standard polymer for biomedical applications.[3,4] Questions regarding the potential immunogenicity of PEG[5,6] and its degradation modes[7,8] have motivated the search for polymers that could serve as substitutes or complements. Among the many polymers studied in this context, which include poly(oligo-(ethylene glycol) methyl ether methacrylate),[9–11] poly(*N*-(2-hydroxypropyl)methacrylamide),[12] polysarcosine,[13] polyvinylpyrrolidone,[14] poly(*N*-acryloylmorpholine),[11] and polyzwitterions,[15,16] PAOx have shown some of the most promising results, with a drug conjugate to treat Parkinson's disease currently in clinical trials.[17]

PAOx are synthesized by cationic ring-opening polymerization (CROP). Chemical and physical versatility is provided by variation of the side chain of the requisite 2-alkyl/aryl-2-oxazoline monomers, as well as by the use of suitable initiators and terminators for chain-end functionalization.[18–21] Notably, end-capping with appropriately designed terminators enables facile introduction of functional groups that would otherwise be incompatible with CROP. Moreover, end-capping with species such as styrenics,[22–25] acrylates,[26–30] and methacrylates[27,30–32] provides macromonomers (MM) that can be used to form graft and comb-like copolymers in subsequent graft-through polymerizations. For instance, RAFT copolymerization of methyl methacrylate and an ω-methacrylated poly(2-ethyl-2-oxazoline) (PEtOx) MM afforded pH- and temperature-responsive graft copolymers.[31] Nonetheless, attempts to prepare PEtOx-based bottlebrush polymers (BBPs) via free radical, RAFT, or nitroxide-mediated polymerizations revealed a steric crowding effect, preventing the formation of BBPs with degrees of polymerization (DP) > 25.[29]

Graft-through ring-opening metathesis polymerization (ROMP) has been applied to the synthesis of a wide range of polymeric architectures including bottlebrush and dendronized polymers.[33–39] ROMP of norbornene-functionalized MMs using ruthenium initiators is particularly suited for the synthesis of side-chain functional polymers with controllable molar masses and low dispersities.[12,39–42] Cross-linking of living BBPs results in another unique nanoarchitecture: the brush-arm star polymer (BASP).[43] BASPs feature a dense

unimolecular micelle-like structure, with tunable core and shell functionalities that may consist of a variety of polymer compositions, as well as therapeutic payloads or imaging agents covalently bound at the core-shell interface. Such features have been exploited to afford two- and three-miktoarm[44,45] as well as PEG-based[46] BASPs with promising properties for drug delivery and imaging applications, including magnetic resonance imaging (MRI) and near-infrared fluorescence (NIRF) imaging.[43,47]

To date, BBPs and BASPs intended for biomedical applications have primarily been derived from norbornene-terminated PEG MMs. Given the significant interest in PAOx as alternatives to PEG, we sought to investigate the properties of PAOx-based BBPs and BASPs synthesized via graft-through ROMP. Herein, we present the design and synthesis of ROMP-compatible PAOx-based MMs (Scheme 1A). Specifically, termination of growing PEtOx chains with a norborneneacid (**X**) or a norbornene-alkyne-acid (**Y**) afforded linear and bivalent MMs **MM1** and **MM2**, respectively. We demonstrate the efficient synthesis of BBPs from **MM1** using ROMP (Scheme 1B). In addition, **MM2** was conjugated to an azide-containing bis-spirocyclohexyl nitroxide (**N_3-chex**) via coppercatalyzed azide-alkyne cycloaddition (CuAAC) to produce **MM3**, which was subsequently used for the synthesis of PEtOx-based BASP organic-radical contrast agents (BASP-ORCAs; Scheme 1C) that could serve as alternatives to metal-containing MRI contrast agents and to previously reported PEG-based ORCAs.[47–50]

PEtOx was prepared following previously reported optimal conditions (microwave irradiation at 140 °C in acetonitrile),[51] with methyl tosylate as the initiator and a monomer-to-initiator ratio of 30. The polymerization was terminated by addition of either **X** or **Y**, providing **MM1** or **MM2**, respectively (Scheme 1, see Supporting Information for details). Size-exclusion chromatography (SEC) traces of both MMs showed a monomodal molar mass distribution with $Đ < 1.2$ (Figures 1 and S7). The successful end-functionalization of both MMs was confirmed by matrix-assisted laser desorption/ionization time-of-flight (MALDI-ToF) mass spectrometry. The spectra showed a major species with the targeted mass:charge ratio, that is, with methyl and norbornene-based groups as the α and ω chain ends, respectively (Figures S1 and S2). A second population of lower intensity was observed in both spectra; it could be assigned to proton-initiated PEtOx, potentially arising from trace water or chain transfer.[52–54] Nevertheless, the norbornene group is present in both species, making them suitable for ROMP. ^{1}H NMR further confirmed the presence of the desired end-groups (Figures S3 and S4). The integration values for the end-group signals of each MM, at 2.9 ppm for the α methyl group and at 6.2 ppm for the ω norbornene olefin, slightly differed from the theoretical 3:2 ratio due to the presence of the aforementioned proton-initiated polymer chains. Number-average molar mass values calculated from ^{1}H NMR (M_n,NMR) by ω end-group analysis were 2700 and 3080 g mol^{-1} for **MM1** and **MM2**, respectively. These values are in close agreement with the expected values. Table S1 provides a summary of the characterization data for these MMs.

Next, we investigated ROMP of these PEtOx MMs. First, **MM1** was dissolved in THF and exposed to Grubbs 3rd-generation bispyridyl complex (**G3**) at a MM/**G3** ratio (i.e., targeted degree of polymerization, DP_{theo}) of 10:1 at room temperature. Samples of the reaction were quenched at predetermined time points by addition of excess ethyl vinyl ether (EVE). SEC

analysis revealed that full conversion was achieved within 10 min (Figure S8). **PEtOx** BBPs with varying DP_{theo} (10, 25, and 50) were prepared, and SEC analyses showed high conversion in all cases, with the expected $M_{n,SEC}$ increase and $Đ < 1.2$ (Figure 1). Further characterization by ^{1}H NMR (Figure S9) shows the characteristic **PEtOx** signals (3.4, 2.3, and 1.05 ppm) and the appearance of signals from the polynorbornene olefin backbone (5.5 and 5.8 ppm), while the norbornene alkene signal from **MM1** (6.2 ppm) is no longer visible.

After successful ROMP of linear **MM1**, we investigated the synthesis of functional polymers derived from bivalent **MM2**, which features a PEtOx chain and a pendant alkyne for the conjugation of an azide of interest by CuAAC.[55] As opposed to copolymerization of two monomers, the use of bivalent MMs ensures that exactly one of each side chain group (e.g., polymer and azide of interest) is attached onto each repeating unit of the resulting BBP. It also sets the location of the smaller group (in this case, the azide) within the core of the BBP architecture.[56] To illustrate this concept, we conjugated an azide-functionalized spirocyclohexyl nitroxide (**N_3-chex**, Scheme 1) to **MM2** by CuAAC, thus providing **MM3**. **MM3** was characterized using MALDI-ToF MS, SEC, and electron paramagnetic resonance (EPR) spectroscopy. The SEC traces confirmed that the structure of the polymer backbone after the CuAAC reaction remains unchanged, conserving its narrow molar mass distribution ($Đ = 1.13$; Figure S7). MALDI-ToF MS validated the quantitative functionalization of **MM2**, with the main population observed having identical theoretical and experimental *m/z* values (Figure S5). These findings were further corroborated by EPR (Figure 3A, vide infra), where the measured spin concentration was >95%.

PEGylated dendrimers, bottlebrush polymers, and BASPs carrying chex have been used as redox probes and highly sensitive ORCAs for MRI.[47,57–59] In particular, PEGylated BASP-ORCAs featuring chex have exceptionally high transverse relaxivities that enable T_2-weighted tumor imaging in vivo.[58] Here, we sought to prepare PEtOx-based BASP-ORCAs for comparison to our previously reported PEGylated BASP-ORCAs. Following the brush-first ROMP approach,[43] **MM3** (7 or 10 equiv) was exposed to **G3** (1 equiv) for 30 min to yield living BBPs with DP_{theo} = 7 or 10, respectively. Then, N = 20 or 30 equiv of bisnorbornene acetal cross-linker (**AcetalXL**) were added, and the mixtures were allowed to react for 6 h while stirring. Following quenching with EVE, the samples were characterized by NMR and SEC. ^{1}H NMR shows the relevant PEtOx signals (3.4, 2.3, and 1.05 ppm) and the absence of the norbornene alkene signal from **MM3** (6.2 ppm) after the formation of **BBP1** and the respective **BASPs** (Figure S10). SEC analysis revealed good conversion for both the MM-to-BBP and the BBP-to-BASP steps (Figure 2). The $M_{n,SEC}$ values for the N = 20 BASPs with DP_{theo} = 7 or 10 were similar (5.9 or 5.0 × 10^5 g mol^{-1}, respectively). Conversely, by keeping the BBP DP_{theo} constant (i.e., 7), but increasing N from 20 to 30, the $M_{n,SEC}$ underwent an approximately 2-fold increase (5.9 to 10.8 × 10^5 g mol^{-1}), showcasing the influence of N on the size of the resulting BASPs. This trend was further confirmed by dynamic light scattering (DLS) and transmission electron microscopy (TEM, Figure S11), where the largest BASP diameter ($D_{h,DLS}$ = 27 ± 9 nm, D_{TEM} = 54 ± 10 nm) was observed for N = 30, compared to its N = 20 BASP analogue ($D_{h,DLS}$ = 21 ± 6 nm, D_{TEM} = 47 ± 7 nm; Figure 3C). It should be noted that the larger D_{TEM} compared to $D_{h,DLS}$ is due to aggregation of the BASPs during TEM sample preparation.

EPR was used to confirm and quantify the presence of chex in these polymers. The normalized EPR spectra for **MM3**, its corresponding DP_{theo} = 10 BBP, and three different BASP-ORCAs are shown in Figure 3A. Consistent with previous reports,[47,57,58] the peaks in the spectra for BBPs and BASP-ORCAs are significantly broadened compared to those for the MM precursor. Computational analyses of these spectra reveal that the fast-moving nitroxide radicals of **MM3** are restricted in motion near the polynorbornene backbone of the BBP and BASP-ORCAs (Figure S12). For BASP-ORCAs, the signal broadening is more apparent due to the drastically reduced freedom of motion of the nitroxides, as these are trapped near the rigid core of the BASP. These results are similar to what was reported for PEG-based BASP-ORCAs.[47,57,58] In all cases, the measured spin concentrations were very high (>85%).

To evaluate the potential of these polymers as metal-free MRI contrast agents, their longitudinal (r_1) and transverse (r_2) relaxivities were measured by collecting phantom images (Figure 3B) at various polymer concentrations using a 7 T MRI scanner. The paramagnetic nitroxide radicals provide MRI contrast by shortening the longitudinal (T_1) and transverse (T_2) relaxation times of neighboring water molecules. The per nitroxide r_1 values obtained for this family of polymers ranged from 0.14 to 0.19 mM^{-1} s^{-1}, showing minimal variation when the polymer architecture was changed from **MM3** (0.14 mM^{-1} s^{-1}) to BBP and BASP (Figure 3C). Nevertheless, r_2 underwent a significant increase from 0.17 (for **MM3**) to 0.58 (for **BBP1**) and further rose to 1.83–2.28 mM^{-1} s^{-1} for the BASPs, with the largest r_2 observed for the BASP synthesized using N = 30. This large r_2 value leads to significant darkening (i.e., negative contrast) of phantom images of the BASP-ORCA solutions compared to **MM3** and *BBP1* (Figure 3B). Compared to the common model nitroxide 3-carbamoyl-PROXYL (3-CP), the r_2 values obtained from the PEtOx-based BASPs are 11–13.5 larger[47] and are up to 7.5-fold larger than a recently reported polyurethane-based ORCA.[60] Nevertheless, these values are still below those of analogous PEG-based BASP-ORCAs (4.67 mM^{-1} s^{-1}).[47] Apart from the absolute relaxivity, the r_2/r_1 ratio is also crucial for achieving optimal T_2-weighted MRI contrast.[61] Notably, the r_2/r_1 ratios of the PEtOx-based BASPs are comparable to those of reported PEG-based BASP-ORCAs. Further screening of parameters such as BBP DP_{theo} and cross-linker equivalents N could potentially positively impact their relaxivities. Never-theless, the results reported here already make PEtOx-based BASPs competitive with PEG-based BASPs, the latter of which have the highest-known r^2 values for organic contrast agents, and should motivate their further investigation in vivo.

In this work, a versatile approach for the synthesis of functional PEtOx-based polymers with complex nanoarchitectures by ROMP is described. Novel norbornene-terminated PEtOx MMs were designed by exploiting the termination step of CROP. ROMP of these MMs led to a variety of well-defined BBPs, with the possibility to introduce functionalities by using bivalent MMs and CuAAC. This strategy allowed the formation of BASPs containing stable chex nitroxides that can potentially be used as ORCAs for MRI. The evaluation of the magnetic properties of these structures showed relaxivity values far exceeding those of model nitroxides and polyurethane-based ORCAs. These results show the suitability of our

PEtOx-based BASP-ORCAs as metal-free MRI contrast agents and their potential for further development as an alternative to the previously reported PEG-based MRI probes.

Supplementary Material

Refer to Web version on PubMed Central for supplementary material.

ACKNOWLEDGMENTS

G.G.A. thanks the Mexican National Council for Science and Technology (CONACyT) for a doctoral research scholarship and the Karlsruhe House of Young Scientist (KHYS) for a research travel grant. We thank the NIH-NCI (1R01CA220468-01 for J.A.J. and A.J.), the NIH (U01-NS090451 for A.J.), and the National Science Foundation (Graduate Research Fellowship for H.V.-T.N.) for support of this research. This work was supported in part by the Koch Institute Support (core) Grant P30-CA14051 from the National Cancer Institute. G.D. acknowledges financial support by the German Federal Ministry of Education and Research (BMBF) through the “Molecular Interaction Engineering: From Nature’s Toolbox to Hybrid Technical Systems” program, Funding Code 031A095B.

REFERENCES

(1). Hoogenboom R Poly(2-Oxazoline)s: Alive and Kicking. Macromol. Chem. Phys 2007, 208, 18–25.

(2). Hoogenboom R Poly(2-Oxazoline)s: A Polymer Class with Numerous Potential Applications. Angew. Chem., Int. Ed 2009, 48, 7978–7994.

(3). Knop K; Hoogenboom R; Fischer D; Schubert US Poly(Ethylene Glycol) in Drug Delivery: Pros and Cons as Well as Potential Alternatives. Angew. Chem., Int. Ed 2010, 49, 6288–6308.

(4). Qi Y; Chilkoti A Protein-Polymer Conjugation Moving beyond PEGylation. Curr. Opin. Chem. Biol 2015, 28, 181–193. [PubMed: 26356631]

(5). Schellekens H; Hennink WE; Brinks V The Immunogenicity of Polyethylene Glycol: Facts and Fiction. Pharm. Res 2013, 30, 1729–1734. [PubMed: 23673554]

(6). Raynor JE; Capadona JR; Collard DM; Petrie TA; García AJ Polymer Brushes and Self-Assembled Monolayers: Versatile Platforms to Control Cell Adhesion to Biomaterials. Biointerphases 2009, 4, FA3–FA16. [PubMed: 20408714]

(7). Ulbricht J; Jordan R; Luxenhofer R On the Biodegradability of Polyethylene Glycol, Polypeptoids and Poly(2-Oxazoline)S. Biomaterials 2014, 35, 4848–4861. [PubMed: 24651032]

(8). Pidhatika B; Rodenstein M; Chen Y; Rakhmatullina E; Muehlebach A; Acikgoz C; Textor M; Konradi R Comparative Stability Studies of Poly(2-Methyl-2-Oxazoline) and Poly(Ethylene Glycol) Brush Coatings. Biointerphases 2012, 7, 1–15. [PubMed: 22589044]

(9). Bontempo D; Maynard HD Streptavidin as a Macroinitiator for Polymerization : In Situ Protein - Polymer Conjugate Formation Streptavidin as a Macroinitiator for Polymerization : In Situ Protein - Polymer Conjugate Formation. J. Am. Chem. Soc 2005, 127, 6508–6509. [PubMed: 15869252]

(10). Gao W; Liu W; Christensen T; Zalutsky MR; Chilkoti A In Situ Growth of a PEG-like Polymer from the C Terminus of an Intein Fusion Protein Improves Pharmacokinetics and Tumor Accumulation. Proc. Natl. Acad. Sci. U. S. A 2010, 107, 16432–16437. [PubMed: 20810920]

(11). Morgenstern J; Alvaradejo GG; Bluthardt N; Beloqui A; Delaittre G; Hubbuch J Investigated with Discrete Conjugates : Alternatives to PEGylation Impact of Polymer Bioconjugation on Protein Stability and Activity Investigated with Discrete Conjugates : Alternatives to PEGylation. Biomacromolecules 2018, 19, 4250–4262. [PubMed: 30222929]

(12). Duncan R The Dawning Era of Polymer Therapeutics. Nat. Rev. Drug Discovery 2003, 2, 347–360. [PubMed: 12750738]

(13). Birke A; Ling J; Barz M Polysarcosine-Containing Copolymers: Synthesis, Characterization, Self-Assembly, and Applications. Prog. Polym. Sci 2018, 81, 163–208.

(14). Caliceti P; Schiavon O; et al. Physico-Chemical and Biological Properties of Monofunctional Hydroxy Terminating PVP Conjugated Superoxide Dismutase. J. Bioact. Compat. Polym 1995, 10, 103–120.

(15). Keefe AJ; Jiang S Poly(Zwitterionic)Protein Conjugates Offer Increased Stability without Sacrificing Binding Affinity or Bioactivity. Nat. Chem 2012, 4, 59–63.

(16). Jiang S; Cao Z Ultralow-Fouling, Functionalizable, and Hydrolyzable Zwitterionic Materials and Their Derivatives for Biological Applications. Adv. Mater 2010, 22, 920–932. [PubMed: 20217815]

(17). Sedlacek O; Monnery BD; Mattova J; Kucka J; Panek J; Janouskova O; Hocherl A; Verbraeken B; Vergaelen M; Zadinova M; et al. Poly (2-Ethyl-2-Oxazoline) Conjugates with Doxorubicin for Cancer Therapy : In Vitro and in Vivo Evaluation and Direct Comparison to Poly[N-(2-Hydroxypropyl)-methacrylamide] Analogues. Biomaterials 2017, 146, 1–12. [PubMed: 28892751]

(18). Verbraeken B; Monnery BD; Lava K; Hoogenboom R The Chemistry of Poly(2-Oxazoline)S. Eur. Polym. J 2017, 88, 451–469.

(19). Guillerm B; Monge S; Lapinte V; Robin JJ How to Modulate the Chemical Structure of Polyoxazolines by Appropriate Functionalization. Macromol. Rapid Commun. 2012, 33, 1600–1612. [PubMed: 22760956]

(20). Gil Alvaradejo G; Glassner M; Hoogenboom R; Delaittre G Maleimide End-Functionalized Poly(2-Oxazoline)s by the Functional Initiator Route: Synthesis and (Bio) Conjugation. RSC Adv. 2018, 8, 9471–9479.

(21). Le D; Wagner F; Takamiya M; Hsiao I-L; Gil Alvaradejo G; Straehle U; Weiss C; Delaittre G Straightforward Access to Biocompatible Poly(2-Oxazoline)-Coated Nanomaterials by Polymerization-Induced Self-Assembly. Chem. Commun 2019, 55, 3741.

(22). Voit B; Shevtsova G; Rueda JC; Komber H; Cedron JC Synthesis of New Hydrogels by Copolymerization of Poly(2-Methyl-2-Oxazoline) Bis(Macromonomers) and N-Vinylpyrrolidone. Macro- mol. *Chem. Phys*. 2003, 204, 947–953.

(23). Groß A; Maier G; Nuyken O Synthesis and Copolymerization of Macromonomers Based on 2-Nonyl- and 2-Phenyl-2-Oxazoline. Macromol. Chem. Phys 1996, 197, 2811–2826.

(24). Kobayashi S; Kaku M; Sawada S; Saegusa T Synthesis of Poly(2-Methyl-2-Oxazoline) Macromers. Polym. Bull. 1985, 13, 447–451.

(25). Shimano Y; Sato K; Kobayashi S Synthesis of Novel Macromonomers and Telechelics of Poly(2-Alkyl-2-Oxazoline)S. J. Polym. Sci., Part A: *Polym. Chem*. 1995, 33, 2715–2723.

(26). Christova D; Velichkova R; Goethals EJ Bis-Macro-monomers of 2-Alkyl-2-Oxazolines - Synthesis and Polymerization. Macromol. Rapid Commun. 1997, 18, 1067–1073.

(27). Kobayashi S; Masuda E; Shoda S; Shimano Y Synthesis of Acryl- and Methacryl-Type Macromonomers and Telechelics by Utilizing Living Polymerization of 2-Oxazolines. Macromolecules 1989, 22, 2878–2884.

(28). Miyamoto M; Naka K; Tokumizu M; Saegusa T End Capping of Growing Species of Poly(2-Oxazoline) with Carboxylic Acid: A Novel and Convenient Route To Prepare Vinyl- and Carboxy-Terminated *Macromonomers*. Macromolecules 1989, 22, 1604–1607.

(29). Weber C; Babiuch K; Rogers S; Perevyazko IY; Hoogenboom R; Schubert US Unexpected Radical Polymerization Behavior of Oligo(2-Ethyl-2-Oxazoline) Macromonomers. Polym. Chem 2012, 3, 2976.

(30). Shoda S-I; Masuda E; Furukawa M; Kobayashi S Synthesis and Surfactant Property of Copolymers Having a Poly(2-oxazoline) Graft Chain. J. Polym. Sci., Part A: Polym. Chem 1992, 30, 1489–1494.

(31). Weber C; Krieg A; Paulus RM; Lambermont-Thijs HML; Becer CR; Hoogenboom R; Schubert US Thermal Properties of Oligo(2-Ethyl-2-Oxazoline) Containing Comb and Graft Copolymers and Their Aqueous Solutions. Macromol. Symp 2011, 308, 17–24.

(32). Weber C; Becer CR; Guenther W; Hoogenboom R; Schubert US Dual Responsive Methacrylic Acid and O1igo(2-Ethyl-2-Oxazoline) Containing Graft Copolymers. Macromolecules 2010, 43, 160–167.

(33). Le D; Montembault V; Soutif JC; Rutnakornpituk M; Fontaine L Synthesis of Well-Defined ω-Oxanorbornenyl Poly- (Ethylene Oxide) Macromonomers via Click Chemistry and Their Ring-Opening Metathesis Polymerization. Macromolecules 2010, 43, 5611–5617.

(34). Le D; Morandi G; Legoupy S; Pascual S; Montembault V; Fontaine L Cyclobutenyl Macromonomers: Synthetic Strategies and Ring-Opening Metathesis Polymerization. Eur. Polym. J 2013, 49, 972–983.

(35). Johnson JA; Lu YY; Burts AO; Lim YH; Finn MG; Koberstein JT; Turro NJ; Tirrell DA; Grubbs RH Core-Clickable PEG-Branch-Azide Bivalent-Bottle-Brush Polymers by ROMP: Grafting-through and Clicking-To. J. Am. Chem. Soc 2011, 133, 559–566. [PubMed: 21142161]

(36). Nyström A; Malkoch M; Furó I; Nyström D; Unal K;Antoni P; Vamvounis G; Hawker C; Wooley K; Malmström E; et al. Characterization of Poly(Norbornene) Dendronized Polymers Prepared by Ring-Opening Metathesis Polymerization of Dendron Bearing Monomers. Macromolecules 2006, 39, 7241–7249.

(37). Rajaram S; Choi T; Rolandi M; Frechet JMJ Synthesis of Dendronized Diblock Copolymers via Ring-Opening Metathesis Polymerization and Their Visualization Using Atomic Force Microscopy. J. Am. Chem. Soc 2007, 129, 9619–9621. [PubMed: 17636929]

(38). Percec V; Schlueter D Mechanistic Investigations on the Formation of Supramolecular Cylindrical Shaped Oligomers and Polymers by Living Ring Opening Metathesis Polymerization of a 7-Oxanorbornene Monomer Substituted with Two Tapered Monodendrons. Macromolecules 1997, 30, 5783–5790.

(39). Xia Y; Kornfield JA; Grubbs RH Efficient Synthesis of Narrowly Dispersed Brush Polymers via Living Ring-Opening Metathesis Polymerization of Macromonomers. Macromolecules 2009, 42, 3761–3766.

(40). Peer D; Karp JM; Hong S; Farokhzad OC; Margalit R; Langer R Nanocarriers as an Emerging Platform for Cancer Therapy. Nat. Nanotechnol 2007, 2, 751–760. [PubMed: 18654426]

(41). Bielawski CW; Grubbs RH Living Ring-Opening Metathesis Polymerization. Prog. Polym. Sci 2007, 32, 1–29.

(42). Ogba OM; Warner NC; O'Leary DJ; Grubbs RH Recent Advances in Ruthenium-Based Olefin Metathesis. Chem. Soc. Rev 2018, 47, 4510–4544. [PubMed: 29714397]

(43). Liu J; Burts AO; Li Y; Zhukhovitskiy AV; Ottaviani MF; Turro NJ; Johnson JA Brush-First" Method for the Parallel Synthesis of Photocleavable, Nitroxide-Labeled Poly(Ethylene Glycol) Star Polymers. J. Am. Chem. Soc 2012, 134, 16337–16344. [PubMed: 22953714]

(44). Shibuya Y; Johnson JA; Nguyen HV-T Mikto-Brush-Arm Star Polymers via Cross-Linking of Dissimilar Bottlebrushes: Synthesis and Solution Morphologies. ACS Macro Lett. 2017, 6, 963–968.

(45). Burts AO; Gao AX; Johnson JA Brush-First Synthesis of Core-Photodegradable Miktoarm Star Polymers via ROMP: Towards Photoresponsive Self-Assemblies. Macromol. Rapid Commun. 2014, 35, 168–173. [PubMed: 24265215]

(46). Gao AX; Liao L; Johnson JA Synthesis of Acid-Labile PEG and PEG-Doxorubicin-Conjugate Nanoparticles via Brush-First ROMP. ACS *Macro Lett.* 2014, 3, 854–857. [PubMed: 25243099]

(47). Nguyen HVT; Chen Q; Paletta JT; Harvey P; Jiang Y; Zhang H; Boska MD; Ottaviani MF; Jasanoff A; Rajca A; et al. Nitroxide-Based Macromolecular Contrast Agents with Unprecedented Transverse Relaxivity and Stability for Magnetic Resonance Imaging of Tumors. ACS Cent. Sci 2017, 3, 800–811. [PubMed: 28776023]

(48). Mendichovszky IA; Marks SD; Simcock CM; Olsen ØE Gadolinium and Nephrogenic Systemic Fibrosis: Time to Tighten Practice. Pediatr. Radiol 2008, 38, 489–496. [PubMed: 17943276]

(49). Kanda T; Ishii K; Kawaguchi H; Kitajima K; Takenaka D High Signal Intensity in the Dentate Nucleus and Globus Pallidus on Unenhanced T1-Weighted MR Images: Relationship with Increasing Cumulative Dose of a Gadolinium-Based Contrast Material. Radiology 2014, 270, 834–841. [PubMed: 24475844]

(50). McDonald RJ; McDonald JS; Kallmes DF; Jentoft ME; Murray DL; Thielen KR; Williamson EE; Eckel LJ Intracranial Gadolinium Deposition after Contrast-Enhanced MR Imaging. Radiology 2015, 275, 772–782. [PubMed: 25742194]

(51). Wiesbrock F; Hoogenboom R; Leenen MAM; Meier MAR; Schubert US Investigation of the Living Cationic Ring-Opening Polymerization of 2-Methyl, 2-Ethyl, 2-Nonyl, and 2-Phenyl-2-Oxazoline in a Single-Mode Microwave Reactor. Macromolecules 2005, 38, 5025–5034.

(52). Warakomski JM; Thill BP Evidence for Long Chain Branching in Polyethyloxazoline. J. Polym. Sci., Part A: Polym. Chem 1990, 28, 3551–3563.

(53). de la Rosa VR; Tempelaar S; Dubois P; Hoogenboom R; Mespouille L Poly(2-Ethyl-2-Oxazoline)-Block-Polycarbonate Block Copolymers: From Improved End-Group Control in Poly(2-Oxazoline)s to Chain Extension with Aliphatic Polycarbonate through a Fully Metal-Free Ring-Opening Polymerisation Process. Polym. Chem 2016, 7, 1559–1568.

(54). Monnery BD; Shaunak S; Thanou M; Steinke JHG Improved Synthesis of Linear Poly(ethyleneimine) via Low- Temperature Polymerization of 2-Isopropyl-2-oxazoline in Chlorobenzene. Macromolecules 2015, 48, 3197–3206.

(55). Johnson JA; Lu YY; Burts AO; Xia Y; Durrell AC; Tirrell DA; Grubbs RH Drug-Loaded, Bivalent-Bottle-Brush Polymers by Graft-through ROMP. Macromolecules 2010, 43, 10326–10335. [PubMed: 21532937]

(56). Nguyen HVT; Gallagher NM; Vohidov F; Jiang Y; Kawamoto K; Zhang H; Park JV; Huang Z; Ottaviani MF; Rajca A; et al. Scalable Synthesis of Multivalent Macromonomers for ROMP. ACS Macro Lett. 2018, 7, 472–476. [PubMed: 30271675]

(57). Sowers MA; Mccombs JR; Wang Y; Paletta JT; Morton SW; Dreaden EC; Boska MD; Ottaviani MF; Hammond PT; Rajca A; et al. Redox-Responsive Branched-Bottlebrush Polymers for in Vivo MRI and Fluorescence Imaging. Nat. Commun 2014, 5, 1–9.

(58). Nguyen HV-T; Detappe A; Gallagher NM; Zhang H; Harvey P; Yan C; Mathieu C; Golder MR; Jiang Y; Ottaviani MF; et al. Triply Loaded Nitroxide Brush-Arm Star Polymers Enable Metal-Free Millimetric Tumor Detection by Magnetic Resonance Imaging. ACS Nano 2018, 12, 11343–11354. [PubMed: 30387988]

(59). Rajca A; Wang Y; Boska M; Paletta JT; Olankitwanit A; Swanson MA; Mitchell DG; Eaton SS; Eaton GR; Rajca S Organic Radical Contrast Agents for Magnetic Resonance Imaging. J. Am. Chem. Soc 2012, 134, 15724–15727. [PubMed: 22974177]

(60). Garmendia S; Mantione D; Alonso-De Castro S; Jehanno C; Lezama L; Hedrick JL; Mecerreyes D; Salassa L; Sardon H Polyurethane Based Organic Macromolecular Contrast Agents (PU-ORCAs) for Magnetic Resonance Imaging. Polym. Chem 2017, 8, 2693–2701.

(61). Rohrer M; Bauer H; Mintorovitch J; Requardt M; Weinmann HJ Comparison of Magnetic Properties of MRI Contrast Media Solutions at Different Magnetic Field Strengths. Invest. Radiol 2005, 40, 715–724. [PubMed: 16230904]

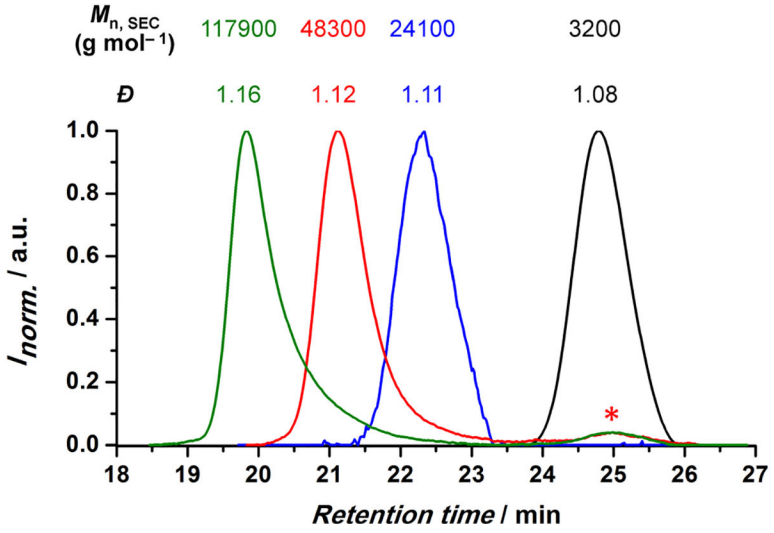

Figure 1.

SEC traces in DMAc of **MM1** and of the BBPs obtained after the graft-through ROMP of **MM1** with THF as solvent and [**MM1**] = 0.05 M, at [**MM1**]/[**G3**] ratios of 10 (blue), 25 (red), and 50 (green). The asterisk (*) denotes trace amounts of unreacted MM.

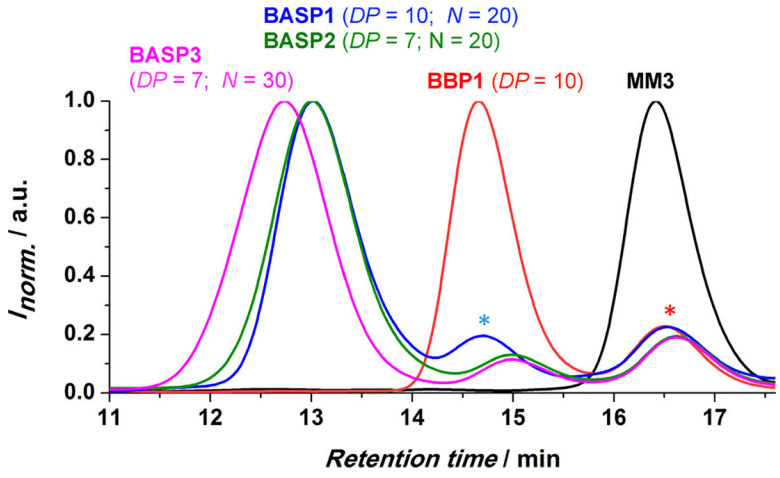

Figure 2.

SEC traces in DMF (0.025 M LiBr) at 60 °C for **MM3**, chex-bottlebrush polymer **BBP1** (with DP_{theo} = 10), and BASP-ORCAs obtained by varying the **MM3**-to-**G3** ratio and the **AcetalXL**-to-**G3** ratio (N). Red "*" and blue "*" denote residual unreacted MM and BBP, respectively.

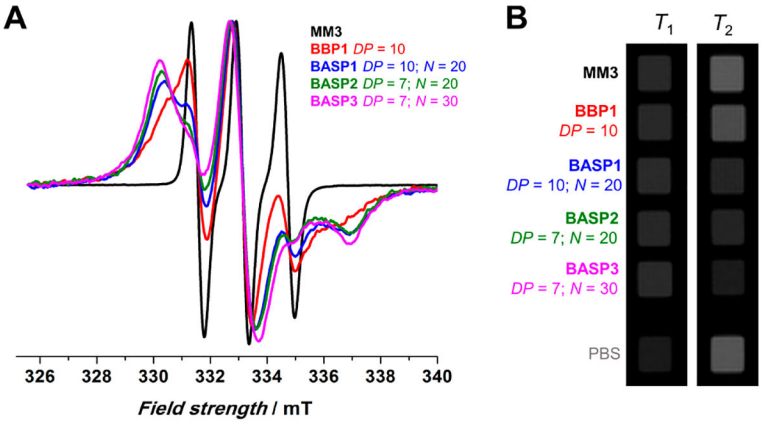

C

	DP	*N*	r_1 mM^{-1} s^{-1}	r_2 mM^{-1} s^{-1}	r_2/r_1	$D_{h,DLS}$ nm	D_{TEM} nm	M_n g mol^{-1} (× 10^{-5})	*Đ*
MM3	1	0	0.14	0.17	1.21	-	-	0.053	1.03
BBP1	10	0	0.16	0.58	3.63	10 ± 4	24 ± 5	0.373	1.01
BASP1	10	20	0.19	1.83	9.63	18 ± 4	47 ± 6	5.04	1.19
BASP2	7	20	0.17	1.96	11.53	21 ± 6	47 ± 7	5.89	1.40
BASP3	7	30	0.19	2.28	12.00	27 ± 9	54 ± 10	10.8	1.47
3-CP			0.15	0.17	1.13	-	-	-	-

Figure 3.

(A) EPR spectra of **MM3**, **BBP1** with DP_{theo} = 10, and BASP-ORCAs obtained by varying **MM3**-to-**G3** ratio (DP_{theo}) and cross-linker-to-G3 ratio (*N*). (B) T_1-weighted and T_2-weighted phantom MR images for BASP-ORCAs dissolved in PBS. (C) Characterization data for the various chex-functionalized PEtOx architectures.

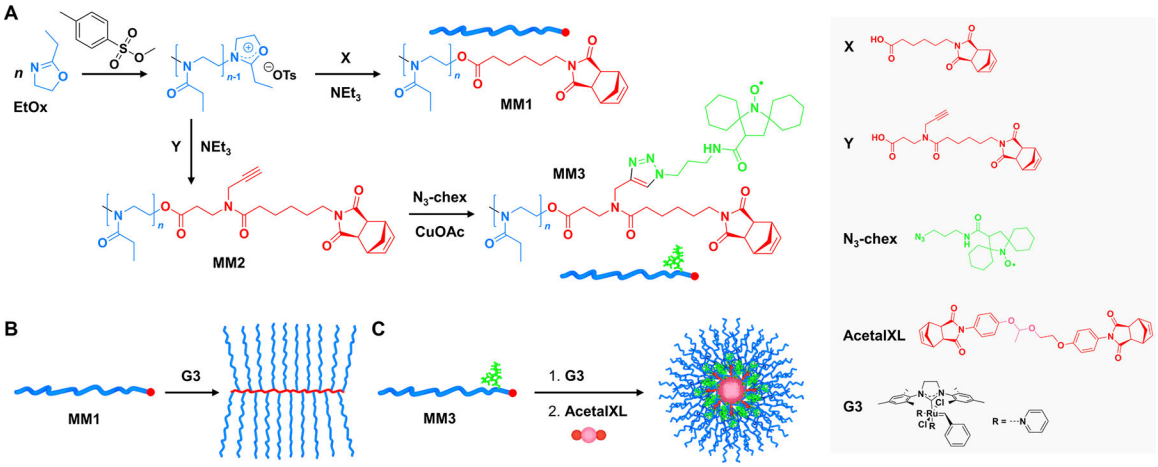

Scheme 1.

(A) Synthesis of PEtOx-Based Norbornene-Terminated MMs; (B) Graft-Through ROMP of Linear MMs (MM1) to Form Bottlebrush Polymers (BBPs); (C) Graft-Through ROMP of Branched MMs (MM3) Functionalized with chex to Provide Living BBPs, and Subsequent Addition of Cross-Linker AcetalXL to Yield PEtOx-Based BASP-ORCAs